Prediction of the Pressure Drop Through Micromachined Particle Filters

Joon Mo Yang*, Xing Yang**, Chih-Ming Ho* and Yu-Chong Tai**

*Mechanical and Aerospace Engineering Department, University of California, Los Angeles
420 Westwood Plaza, Los Angeles, CA90095, U.S.A.
**Caltech Micromachining Laboratory, Electrical Engineering Department, 136-93
California Institute of Technology, Pasadena, CA91125, U.S.A.

ABSTRACT

Micro-filters are fabricated using MEMS technology, and both measurements and numerical calculations are carried out in order to estimate the power requirement in a micron-size particle collection process using the micro-filter. In order to numerically predict the pressure drop through the micro-filter, we focus on the characterization of the geometrical factors, such as internal profile of the filtering hole and the hole dimension. The surface slip is also considered. It is found that the pressure drop through the micro-filter is strongly dependent upon the internal profile of the filtering hole and that the surface-slip is not dominant in determining the pressure drop. When the size of the hole is accurately measured and the internal profile of the filtering hole is correctly modeled, the calculated pressure drop shows good agreement with the measured pressure drop. From the numerical calculation, a formula is proposed which can accurately predict the pressure drop through the micro-filter.

Keywords: micro-filter, pressure drop

INTRODUCTION

A particle collection system is composed of a filter and a suction fan. In order to collect micro-size particles or biological agents from the air, the filter should have an array of micron-size holes, and micromachined membranes with perforations are ideal candidates for this purpose. Recently, micro-filters have been reported by several investigators [1,2,3]. The hole size of the reported micro-filter ranges from 1 μm to 12 μm, and the thickness from 1 μm to 3 μm.

In the micro-size particle collection system, it is an important issue to minimize the power requirement of the suction fan. The power requirement can be calculated by multiplying the pressure drop through the micro-filter by the volumetric flow rate. Therefore, in order to design an efficient filter with low pressure drop, an adequate design rule for the pressure drop should be established.

The flow through a micron-size hole is also an interesting topic for a fundamental research. Hasegawa *et al.*[4] measured the pressure drop through a micron-sized hole in a liquid flow and reported an abnormal high pressure drop compared to that predicted from numerical calculations. On the other hand, Yang *et al.*[3] found that the surface slip is not dominant in determining the pressure drop through the micron-thick filter in an air flow.

In this study, we fabricate two kinds of micro-filters. Both measurements and numerical calculations are carried out to predict the pressure drop through the micro-filter. In the numerical calculation, efforts are made to correctly characterize the geometry of the micro-filter. A formula for the pressure drop through the micro-filter is proposed from numerical calculations.

MICRO-FILTER

A detailed fabrication process is shown in Yang *et al.* [3]. First, a layer of 1 μm thick LPCVD silicon nitride is deposited on a silicon wafer. Windows on the backside of the wafers are opened using plasma etching, and the wafers are etched until only 20 μm silicon is left. Next, an array of filtering holes was etched into the silicon nitride layer on the front side of the wafer using reactive ion etching (RIE). Then the wafers were diced and etched to remove the remaining silicon and free the membrane. Fig.1(a) shows the micro-filter obtained by the fabrication process (Hereinafter, this micro-filter is referred to as MS1.) The hole diameter, d, of MS1 is 12 μm with a spacing between the holes, s, of 18 μm, both of which are determined from the mask in the fabrication process.

In order to attain a micro-filter with a smaller hole size, a layer of Parylene C polymer is deposited over the individual dies, and we get MS2 which is shown in Fig.1(b). Yang *et al.*[3] showed that the layer of Parylene C not only enables us to get different hole sizes, but also greatly improves the strength of membrane filter. The hole size of MS2 is measured using a WYKO surface profiler. Fig.2(a) shows an image taken from the WYKO surface profiler. Images of several locations on the micro-filter are

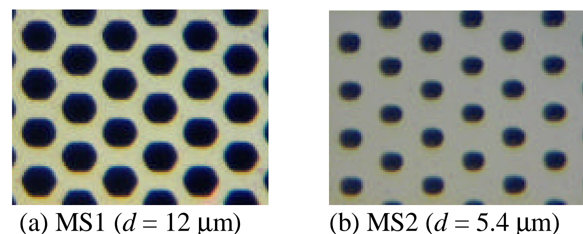

(a) MS1 (d = 12 μm) (b) MS2 (d = 5.4 μm)

Figure 1: Micro-filters fabricated in this study.

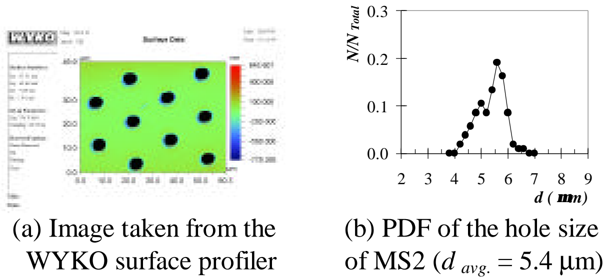

(a) Image taken from the WYKO surface profiler

(b) PDF of the hole size of MS2 ($d_{avg.}$ = 5.4 μm)

Figure 2: Measurement of the hole diameter using a WYKO surface profiler.

taken, and the diameters are measured for more than one hundred holes. Fig.2(b) shows the probability density function (PDF) of the hole diameter of MS2. The average value is found to be 5.4 μm. The thickness of MS2 is measured using an alphastep, and the thickness, *t*, of approximately 3 μm is obtained. It should be noted that, since MS2 is obtained from MS1 as a base filter, the spacing between the holes of MS2 is the same as that of MS1 (*s* = 18 μm).

Table 1 summarizes the micro-filters fabricated in this study. The Knudsen number of each micro-filter is 0.006 and 0.013, which indicate the surface slip is not dominant in this case[3].

The fabricated micro-filter has a size of 10.9 mm x 10.9 mm, and is composed of a filtering region and a non-filtering region. The filtering region has a size of 8 mm x 8 mm. The non-filtering region is basically a silicon wafer with a thickness of 500 μm.

MEASUREMENT

The pressure drop through the micro-filter is measured in a small wind tunnel specially designed for this purpose. The wind tunnel is made of plexiglass and has a 30 cm long square test section of 8 mm x 8 mm. The cross-sectional area is determined so that the non-filtering region of the micro-filter would not be exposed to the test section of the wind tunnel. At 15 cm downstream from the contraction is a notch into which a micro-filter can be inserted.

The volumetric flow rate is determined by measuring the static pressure upstream and downstream of the contraction of the wind tunnel. The static pressure is measured by using a MKS Baraton differential pressure transducer with a resolution of 0.01 Pa. Solving the continuity and the Bernoulli equation, we can calculate the volumetric flow rate and the average velocity at the inlet of the test section. The pressure drop through the micro-filter is measured by using a manometer with a resolution of 1.5 Pa. The measured pressure drop as a function of the flow rate is shown in Fig.7.

	d (μm)	*s* (μm)	*t* (μm)	Kn_d
MS1	12	18	1	0.006
MS2	5.4	18	3	0.013

Table 1: Dimensions of the micro-filters.

NUMERICAL CALCULATION

The computational domains are constructed based on the measured hole size and the geometry of the micro-filter. Basically, the micro-filter is composed of an array of micron-size holes. Since the boundary between the holes has a hexagonal shape (See Fig.1), the micro-filter can be regarded as a conglomeration of small hexagonal regions. Therefore, the hexagonal domain with one hole as shown in Fig.3(a) represents the flow field around the micro-filter (Computational Domain 1: CD1). The 3-dimensional domain can be simplified to an axisymmetric domain as shown Fig.3(b) (CD2). In the axisymmetric domain, *s* is determined so that the opening factor, ***b***, would be the same as that in the 3-dimensional domain. Fig.3(c) shows the internal profile of the hole in CD1 and CD2.

Fig.4(a) and (b) show SEM side view pictures of MS1 and MS2, respectively, after intentionally breaking the two micro-filters. It can be seen that the internal profile of the filtering hole is not straight, which indicates that the profile shown in Fig.3(c) should be re-modeled. As shown in the previous section, reactive ion etching (RIE) is used to etch away the silicon nitride membrane to make the filtering holes. The RIE process is used for anisotropic etching, and ideally it would be a straight profile of the filtering hole, as

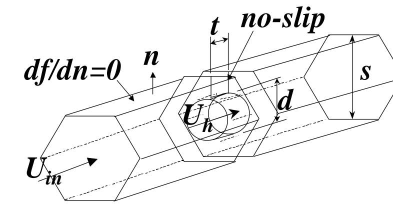

(a) 3-dimensional domain (CD1)

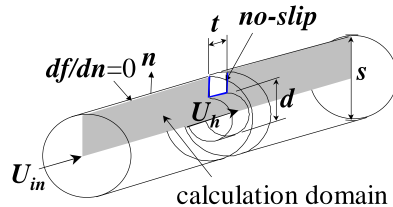

(b) axisymmetric domain (CD2)

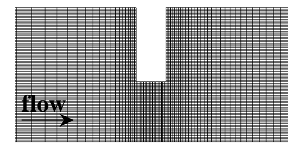

(c) Internal profile of the filtering hole for CD1 and CD2

Figure 3: Calculation domain (CD1 & CD2) and boundary conditions with straight internal profile of the filtering hole.

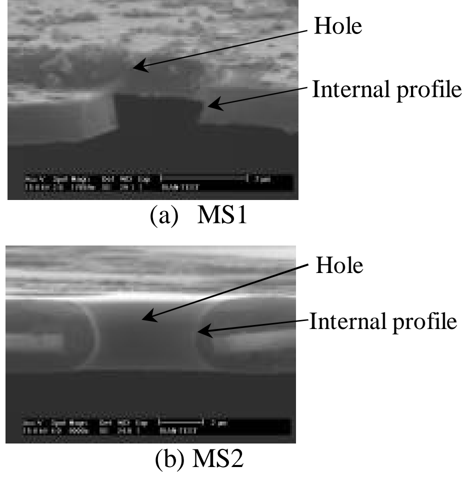

(a) MS1

(b) MS2

Figure 4: SEM picture of the internal profile of the filtering hole.

shown by the dashed line in Fig.5. May *et al.*[5] have extensively studied the internal profile in the RIE process. They showed that the internal profile depends on various plasma parameters. In this study, the internal profile of the hole is observed to be an elliptical shape, and *a/b* is found to be 0.5 (See Fig.4(a) and Fig.5). Based on this consideration, we construct CD3 as shown in Fig.6(a) for MS1. After the Parylene C is conformally deposited on the surface of the silicon nitride membrane (MS2), the internal profile of the hole can be assumed to be as shown in Fig.6(b) (CD4). Also see Fig.4(b).

The numerical calculations are carried out for all four computational domains (CD1~CD4). We assume a laminar flow and use a no-slip boundary condition at the surface of the micro-filter and a symmetry boundary condition at the boundary between the holes as shown in Fig.3. A Computational Fluid Dynamic Research Corporation (CFDRC) software is used to perform calculations.

In the case of MS2, the slip boundary condition is also used (See Table 1). The slip boundary condition can be expressed as,

$$u_w = \pm \frac{2-\boldsymbol{a}}{\boldsymbol{a}} \boldsymbol{l} \left. \frac{du}{dy} \right|_w , \tag{1}$$

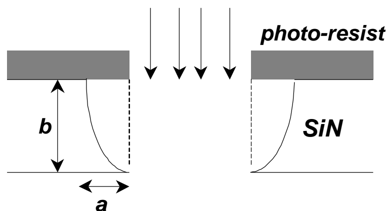

Figure 5: Internal profile of the filtering hole from RIE process (dashed line: ideal case, solid line: real case). *a/b* = 2 (See Fig.4(a)).

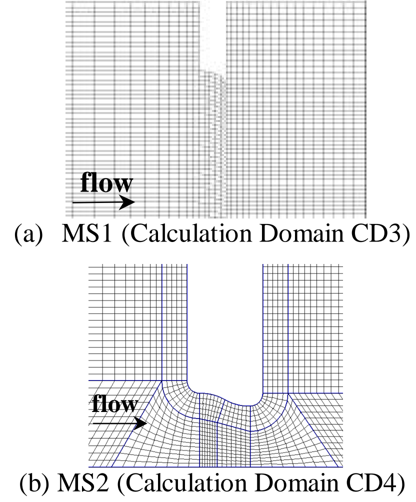

(a) MS1 (Calculation Domain CD3)

(b) MS2 (Calculation Domain CD4)

Figure 6: Internal profile of the filtering hole and the computational domain determined from the SEM picture.

where $\boldsymbol{a}$ is the accommodation constant ($0 < \boldsymbol{a} < 1$) and $\boldsymbol{l}$ is the mean free path of the working fluid.

COMPARISON

Fig.7 shows the measured and the calculated pressure drop through the two kinds of micro-filters (MS1 and MS2). It can be seen that the internal profile of the filtering hole greatly affects the numerically calculated pressure drop, and this effect can be clearly seen especially in the case of MS2. On the other hand, there is only a little difference between the results using the no-slip and the slip boundary conditions (Fig.7(b)). The calculated pressure drop through CD3 and CD4 are in good agreement with the measured pressure drop. Note that the axisymmetric (CD1) and the 3-dimensional calculation (CD2) predict almost the same pressure drop.

This result indicates that, in order to numerically predict the pressure drop through the micro-filter, the geometry should be correctly characterized. In the case of the air flow around a micron-thick filter, surface slip is not dominant in determining the pressure drop.

FORMULA

The pressure drop in CD3 and CD4 is calculated for various values of the parameters ($\boldsymbol{b}$, *t/d* and *Re*). All the calculated results are non-dimensionalized and a formula is established so that all the non-dimensionalized pressure drop would collapse onto a single curve with respect to the Reynolds number:

$$K = \frac{\Delta P}{1/2\, \boldsymbol{r} U_{in}^2} = \boldsymbol{b}^{-2} [3.5 \frac{t}{d} + 3][10.0 \frac{\boldsymbol{nb}}{U_{in} d} + 0.22]. \tag{2}$$

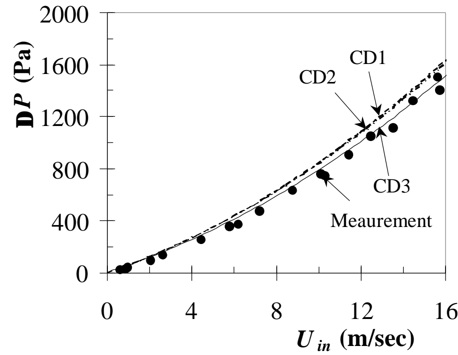

(b) MS1

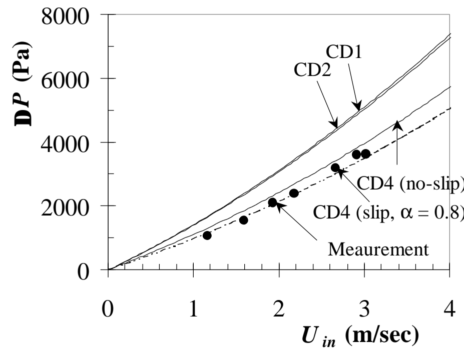

(b) MS2

Figure 7: The measured and the calculated pressure drop through the micro-filter as a function of the inlet velocity.

The formula is verified in Fig.8. For comparison, the measured pressure drop through MS1 and MS2 are also shown. It can be seen that the formula and the measurement show good agreement.

Yang *et al.*[3] also proposed a formula for the pressure drop through the micro-filter from numerical calculations:

$$K = \frac{\Delta P}{1/2\rho U_{in}^2} = \beta^{-2}\left(\frac{t}{d}\right)^{0.28}\left[73.5\frac{\nu\beta}{U_{in}d} + 1.7\right]. \qquad (3)$$

They showed, however, that the pressure drop through the micro-filter predicted by Eq.(3) is much higher than the measured pressure drop. It should be noted that in their calculation, the effect of the internal profile of the filtering hole was not taken into consideration. They established Eq.(3) from numerical calculations in CD2 (Fig.3(b)).

CONCLUSION

In this study, we focus more on the correct characterization of the geometrical factors, such as internal profile of the hole and the hole dimension, than on the micro-fluidic phenomena. It is found that the internal profile of the filtering hole greatly affects the pressure drop

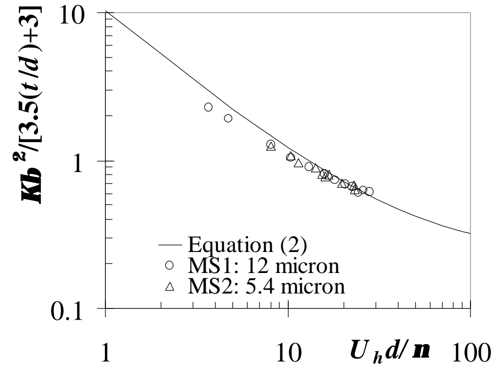

Figure 8: A formula for predicting the pressure drop through the micro-filter, and comparison of the measured pressure drop with the numerically calculated pressure drop.

through the micro-filter. Correct characterization of the geometrical factors enables us to accurately predict the pressure drop through the micro-filter by a numerical calculation based on the Navier-Stokes equation.

ACKNOWLEDGEMENT

This work is supported by the DARPA Microflumes program managed by Naval Ocean Systems Center Contract N66001-96-C-83632. The authors would like to thank Dr.Fan-Gang Tseng, Ms. Ellis Meng and Mr. John D. Mai for their help.

REFERENCES

[1] G.Kittilsland, G.Steme and B. Norden, "A Submicron Particle Filter in Silicon", Sensors and Actuators A: Physical, 23, 904-907, 1990.

[2] C.J.M.van Rijin, M.van der Wekken, W.Hijdam and M.C.Elwenpoek, "Deflection and Maximum Load of Microfiltration Membrane Sieves made with Silicon Micromachining", Journal of Microelectromechanical Systems, 6, No.1, 48-54, 1997.

[3] X.Yang, J.M.Yang, X.Q.Wang, E.Meng, Y.-C Tai and C.-M Ho, "Micromachined Membrane Particle Filters", Proceedings of IEEE, The 11th Workshop on Micro Electro Mechanical Systems, Heidelberg, Germany, 137-142, 1998.

[4] T.Hasegawa, M.Suganuma and H.Watanabe, "Anomaly of Excess Pressure Drops of the Flow Through Very Small Orifices", Physics of Fluids, 9, No.1, 1-3, 1997.

[5] P.W.May, D.Field and D.F.Klemperer, "Simulation of Sidewall Profiles in Reactive Ion Etching", Journal of Physics D: Applied Physics, 26, 598-606, 1993.